Evolution of the Current Density Profile Associated with Magnetic Island Formation in JT-60U

T. Oikawa, A. Isayama, T. Fujita, T. Suzuki, T. Tuda, and G. Kurita

Japan Atomic Energy Research Institute, 801-1 Mukouyama, Naka-machi, Naka-gun, Ibaraki-ken 311-0193, Japan

(Received 9 July 2004; published 1 April 2005)

Evolution of the current density profile associated with magnetic island formation of an $m/n = 2/1$ tearing mode was measured using a motional Stark effect (MSE) diagnostic for the first time in the JT-60U tokamak. With the island growth, the current density profile turned flat at the radial region of the island, followed by an appearance of a hollow structure. As the island shrank, the flat region became narrower, and it finally diminished after the disappearance of the island. The fluctuation of the local poloidal magnetic field from MSE showed a strong correlation with a slow island rotation. This indicates that the observed deformation in the current density profile is localized at the island O point.

DOI: 10.1103/PhysRevLett.94.125003 PACS numbers: 52.55.Fa, 52.35.Py

Tearing modes and magnetic islands [1] are fundamental physical phenomena in magnetized plasmas. In a low temperature plasma, tearing modes are believed to be mainly driven by the current density gradient. In a collisionless regime, once an initial island is produced, neoclassical tearing modes (NTMs) can grow due to a helical deficit in the bootstrap current in the island O point [2]. Whereas other global magnetohydrodynamic (MHD) instabilities [3] and microturbulence trigger [4] are proposed as the origin of a seed island, the classical onset of tearing modes is also reported for NTMs in the DIII-D tokamak [5]. The current density profile plays a key role in the onset and evolution of tearing modes. On the TEXT tokamak, a profile of the magnetic fluctuation due to a classical tearing mode was measured using a heavy ion beam probe [6]. Measurements using a Faraday rotation diagnostic were also reported from the TEXTOR tokamak [7] and reversed field pinch plasmas [8]. However, previous studies on NTMs in high-temperature plasmas were based on external measurements of magnetic fluctuations and/or correlations with internal electron temperature fluctuation measurement. In this Letter, we report the first observation of the current profile evolution associated with magnetic island formation during a tearing mode where the neoclassical drive dominates.

A neutral beam (NB) heated H-mode discharge with an $m/n = 2/1$ tearing mode was investigated in JT-60U (Fig. 1). Here, m and n are poloidal and toroidal mode numbers, respectively. The vacuum toroidal magnetic field at the plasma center B_{t0} is 3.62 T, the plasma current I_p is 1 MA, and the safety factor at the flux surface with 95% of the normalized poloidal flux q_{95} is 6.6. Neutral beam injection of 15 MW at a beam energy of 85 keV started at $t = 3.0$ s. As shown in Fig. 1(a), the $n = 1$ magnetic perturbation appeared when the normalized beta β_N reached ~ 1 at $t \sim 3.3$ s. Here, β_N is defined as $\beta_N \equiv \beta_t \times a[\mathrm{m}]B_{t0}[\mathrm{T}]/I_p[\mathrm{MA}]$, where β_t is the toroidal beta or the ratio of the plasma pressure to the pressure of the toroidal magnetic field and a is the horizontal plasma minor radius. Electron cyclotron emission (ECE) radiometry with a sampling time of 20 μs shows a corresponding perturbation in the electron temperature $\tilde{T}_e$ around the $q = 2$ surface (shown in Fig. 3 below). Time evolutions of the frequency and amplitude at the peak of the $\tilde{T}_e$ spectrum for an ECE channel located just outside the $q = 2$ surface (the normalized minor radius $\rho \sim 0.4$) are shown in Figs. 1(b) and 1(c), respectively. The $m/n = 2/1$ tearing mode grew during $t = 3.3$–3.6 s and saturated. The magnitude of the tearing mode began to decrease at $t \sim 4.4$ s and disappeared at $t \sim 4.8$ s spontaneously. Figure 2 shows a contour of fluctuation amplitude of the electron temperature $\tilde{T}_e/T_e$ at the island rotation frequency. The peaks of the $\tilde{T}_e/T_e$ profile indicated by white or light gray areas indicate the inner and outer edges of the island when the O point of the rotating island is situated at the ECE viewing chord, which lies $\sim$10 cm above the equatorial plane on the outboard side (lower toroidal magnetic field side). The island half-width expanded from $\sim$4 cm at $t = 3.35$ s to $\sim$9 cm at $t = 3.6$ s. The inner peak deviated from the ECE viewing range at $t \sim 3.5$ s due to the island growth. The outward shift of the island center during $t = 3.3$–3.6 s resulted from the Shafranov shift associated with the in-

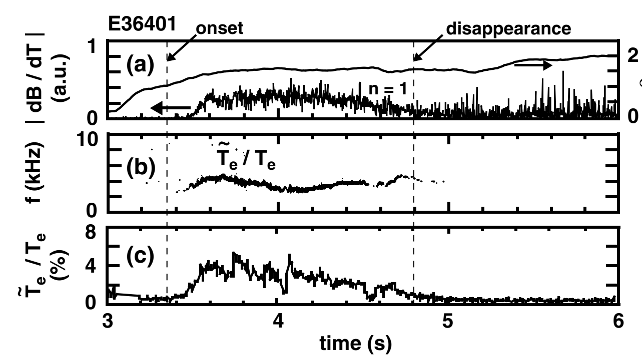

FIG. 1. Time history of an $m/n = 2/1$ tearing mode discharge E36401. (a) The normalized beta β_N and $n = 1$ magnetic perturbation at the wall (in time derivative), (b) frequency spectrum of electron temperature perturbation $\tilde{T}_e$ measured at $\rho \sim 0.4$ by ECE, and (c) amplitude of $\tilde{T}_e/T_e$ at the frequency of the spectrum peak in (b).

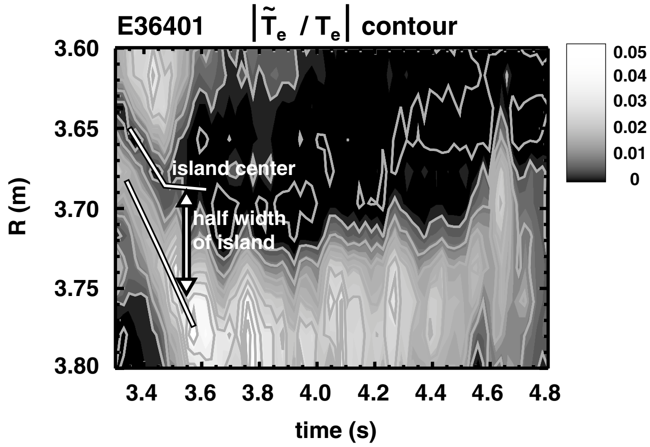

FIG. 2. Contour of fluctuation amplitude of the electron temperature $\tilde{T}_e/T_e$ at the frequency of the spectrum peak. Evolutions of the O point and outer edge of the island structure are indicated for the growth phase with the white thick lines.

crease in plasma beta. The island spontaneously began to shrink at $t \sim 4.4$ s and diminished at $t \sim 4.8$ s.

The current density profile is reconstructed with an MHD equilibrium code using data from a motional Stark effect (MSE) diagnostic [9]. Recently, we have improved our equilibrium code to reproduce small and spatially localized variation in the current density profile. A spline function on the normalized minor radius has been implemented for the current density profile, in addition to polynomial functions on the poloidal flux. Thus, our MHD equilibrium code is capable of reconstructing small changes in the MSE signals.

Figure 3 shows evolutions of radial profiles of the current density $j(\rho)$ and safety factor $q(\rho)$ deduced through equilibrium reconstruction with the MSE data. When the $m/n = 2/1$ tearing mode appeared at $t \sim 3.3$ s, $j(\rho)$ began to decrease and flatten around the $q = 2$ surface located at $\rho = 0.27$ as shown at $t = 3.55$ s, with the island extended to $\rho = 0.18$–0.39. The flat region around the $q = 2$ location became wider at $t = 3.7$ s. In the saturation phase ($t = 3.6$–4.4 s), a hollow structure was formed at the $q = 2$ location as shown at $t = 3.9$ and 4.35 s. With the island shrinking from $t = 4.4$ s, the current density began to increase in the hollow region as observed at and after $t = 4.75$ s. This is considered to be a recovery of the noninductive current in the island O point, as discussed later. Relaxation of a negative electric field generated by the increase in the noninductive current caused the decrease in the current density inside the $q = 2$ surface ($t = 4.75$ and 4.95 s). As a result, the $q = 2$ rational surface moved inward. After the disappearance of the mode at $t \sim 4.8$ s, the hollow structure in $j(\rho)$ disappeared at $t = 5.55$ s. The disappearance of the $m/n = 2/1$ tearing mode is considered to result from the inward shift of the $q = 2$ surface. Four MSE channels are used in reconstructing the structure of the island region when the island fully evolved, as shown at $t = 3.55$ s of Fig. 3. The temporal change in the current density in the island region is larger than a typical error due to the statistical noise as shown at $t = 3.7$ s. Thus, the spatial variation of the current density in the island region can be well resolved.

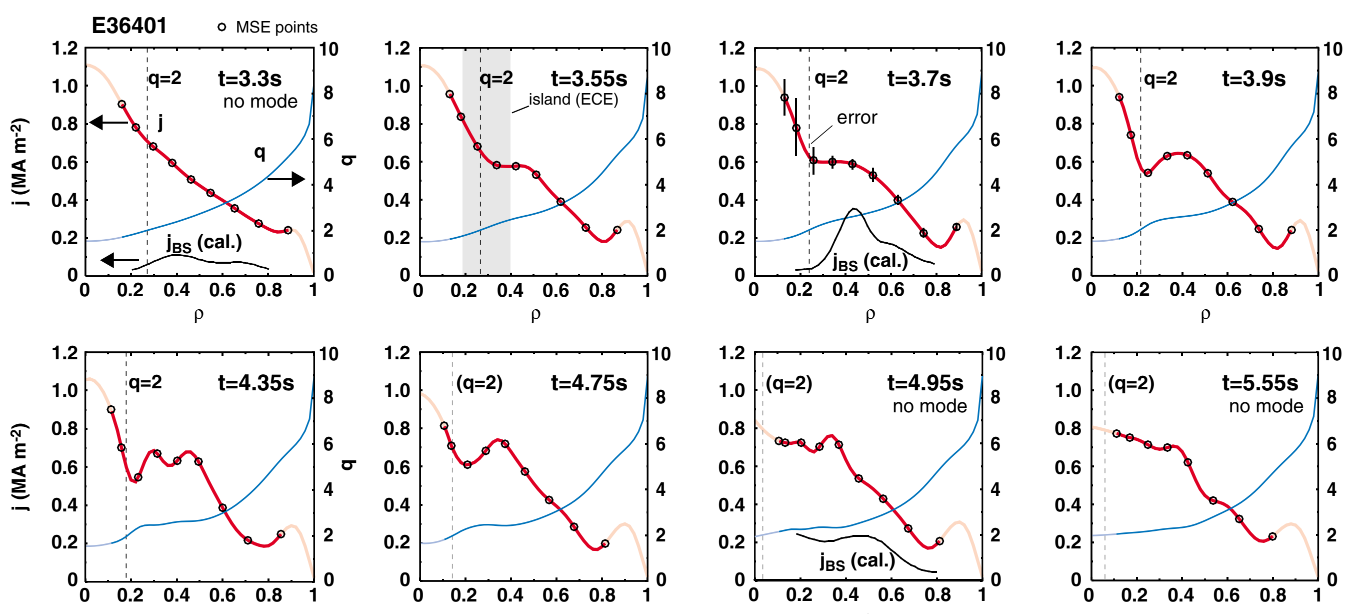

FIG. 3 (color online). Evolutions of the measured current density j and safety factor q profiles in E36401. The open circles indicate the MSE spatial points. A typical error in $j(\rho)$ due to the statistical noise is shown at $t = 3.7$ s. Radial profiles of the calculated bootstrap current density j_{BS} are shown at $t = 3.3$, 3.7, and 4.95 s. The dashed lines indicate the $q = 2$ locations.

Probable causes for the observed deformation in the current density profile are flattening of the current density gradient owing to a classical tearing mode and/or reduction in the noninductive current. In the discharge mentioned above, the noninductive currents are the bootstrap current and codirectional neutral beam current drive (NBCD). In Fig. 3, radial profiles of the bootstrap current density j_{BS} are calculated at $t = 3.3$ s (just before the mode onset), 3.7 s (during the mode excitation), and 4.95 s (after the disappearance of the mode), based on the measured profiles of the ion temperature T_i, electron temperature T_e, and electron density n_e shown in Fig. 4. In the radial region of the island with small gradients of profiles, the estimated bootstrap current is nearly zero. Since time resolutions for the electron and ion temperature profiles are 25 and 50 ms, respectively, the measured temperatures are averages over a hundred island rotations. Consequently, the flat regions in the temperature profiles are observed to be narrower than the island width identified by the ECE radiometer, and hence finite bootstrap current density is calculated in the island region at $t = 3.7$ s. Here, our calculation of the bootstrap current does not take into consideration an island structure. As a result, radial profiles with a flat region are treated to be uniform poloidally in the calculation, and the effect of finite orbits of trapped particles that lie partly inside and partly outside the island are neglected. Thus, this bootstrap current calculation is not conclusive on the reduction of the bootstrap current in the island O point.

A recent result of a Monte Carlo simulation employing the δf method showed that a significant fraction of the ion bootstrap current survives inside the island O point when the ion banana width is comparable to the island width, and that once the island grows larger the bootstrap current inside the island O point disappears along with a small residual current near the island edge [10]. Thus, reduction of the bootstrap current within the island O point is considered to be a cause for the observed deformation in the current density profile. It was reported that, in DIII-D, the NBCD at a beam energy of 75 keV was reduced as a result of fast ion transport when a large $m/n = 2/1$ island existed [11]. In JT-60U, on the other hand, we have observed that, in the presence of a tearing mode, fast ions injected at 360 keV suffered an anomalous transport but fast ions produced from neutral beam at a lower energy of 80–90 keV were not affected [12]. Therefore it is probable that inside the island O point the flattening of the current density gradient owing to a classical tearing mode and/or the loss of the bootstrap current cause the observed deformation in the current density profile.

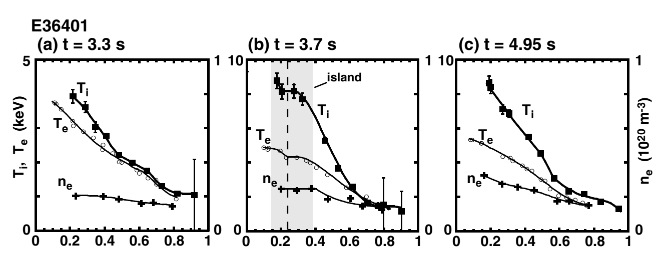

FIG. 4. Radial profiles of the electron and ion temperatures (T_e and T_i) and the electron density n_e at (a) $t = 3.3$ s, (b) $t = 3.7$ s, and (c) $t = 4.95$ s. Here, n_e was measured by YAG (yttrium-aluminum-garnet) laser Thomson scattering, T_i by charge exchange recombination spectroscopy on carbon ions, and T_e by ECE Fourier transform spectroscopy.

Here, we have to recall the following points on the experimental identification of the current density profile. A first point is on the treatment of an island structure in the equilibrium reconstruction. As our equilibrium code does not treat equilibria with an island structure, a reconstructed equilibrium consists of concentric flux surfaces with a single magnetic axis satisfying measurements within a convergence condition in the numerical calculation. The second point is that the MSE measurement is made at a sampling time too slow to identify a rotating island. The MSE signals are digitized every 10 ms and averaged over several tens of milliseconds to reduce the statistical noise. At an effective time resolution, the measurement cannot resolve the variation correlated with the island rotation at ~2–4 kHz in the present case [Fig. 1(b)]. Thus, we cannot determine whether deformation in the current density profile is localized inside the island O point (through processes such as a classical tearing mode and/or the bootstrap current reduction) or occurs uniformly in the poloidal direction (''beltlike'') for some reasons.

In order to investigate the above point, we examined a discharge with a stationary $m/n = 2/1$ tearing mode with intermittent mode lockings. The extent of the island was $\rho \sim 0.5$–0.7. If deformation in the current density profile is localized inside the island O point, the local poloidal magnetic field at the island would represent a temporal variation correlated with the island rotation. In Fig. 5(a), fluctuating electron temperatures at the radii of the island, which were measured in the outboard equatorial plane, show that the island rotation was locked at $t = 7.27$ s and slowly rotated again. At the mode locking, an O point of the $m/n = 2/1$ island structure was located on the outboard equatorial plane. Then, starting to rotate again, an X point moved onto the outboard equatorial plane at $t \sim 7.37$ s. After some rotation, the X point appeared on the outboard at $t = 7.59$ s. Figure 5(b) shows time traces of the MSE polarization angle γ at and near the radial location of the island, where γ is determined from the local toroidal and poloidal magnetic fields. We observed variations in γ correlated with two 180° rotations at $t = 7.4$–7.465 s and $t = 7.535$–7.59 s [indicated by the dashed lines in Fig. 5(b)], which are as slow as the MSE diagnostic can detect the corresponding changes. Since the contribution from the toroidal magnetic field fluctuation is negligibly small in a tokamak, the variations in the MSE signals represent the perturbed poloidal magnetic fields. The

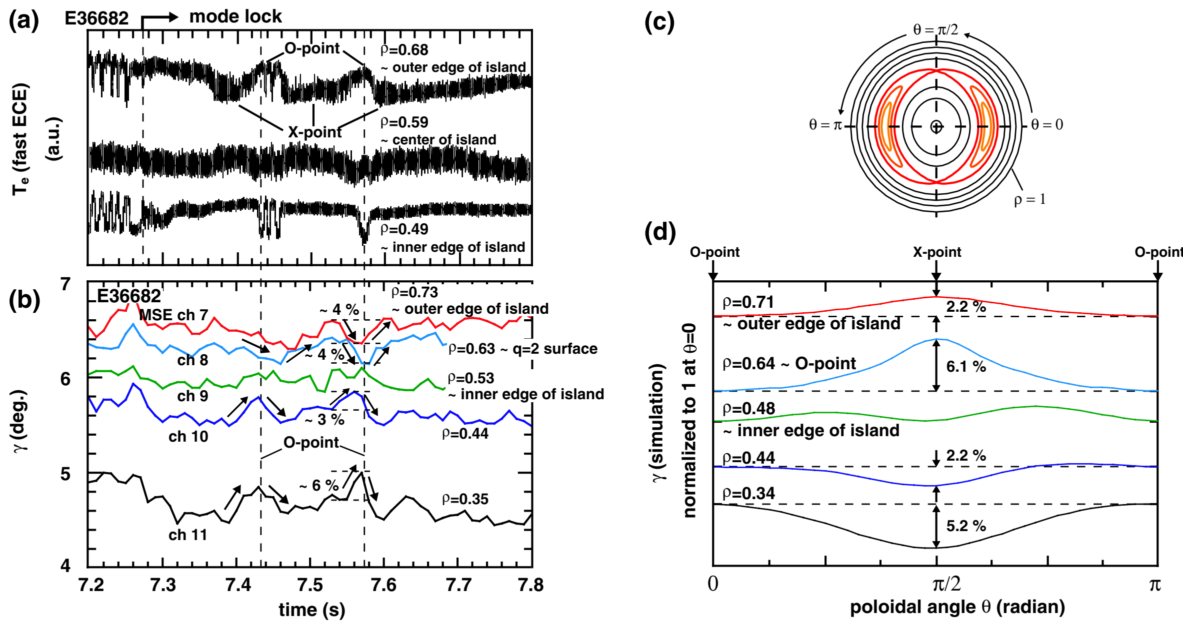

FIG. 5 (color online). Time evolutions of a discharge E36682 with a stationary $m/n = 2/1$ tearing mode with a saturated island structure at $\rho \sim 0.5$–0.7: (a) the fluctuation of electron temperatures at the inner and outer edges of island and the O point and (b) MSE polarization angles γ around the island structure ($\gamma = 0$ when the poloidal magnetic field is zero). A classical tearing mode simulation reproduces the $m = 2/n = 1$ island at $\rho = 0.48$–0.71. (c) Contour of the helical poloidal flux, and (d) calculated γ for the magnetic field along the poloidal direction at the radii corresponding to the MSE points in (b), where the values are normalized at $\theta = 0$.

time lag between the ECE and MSE due to different spatial locations is negligibly small (several milliseconds) for the observed island rotations. At $\rho = 0.35$ and 0.44, the measured γ increased with a change from the X point to the O point and decreased with a change from the O point to the X point. At and outside the radial location near the $q = 2$ surface, γ behaved in the opposite manner. Little change was observed at $\rho = 0.53$ (near the inner island edge). This observation has been validated with a classical tearing mode simulation using a nonlinear resistive MHD code [13]. The $m/n = 2/1$ island structure at $\rho = 0.48$–0.71 is reproduced as shown in Fig. 5(c), where an O point stays at the $\theta = 0$ plane. Figure 5(d) shows calculated γ for the magnetic field along the poloidal direction at the same radii in Fig. 5(b). The variation in γ between an O point and an X point at each radial location agrees reasonably with the observation. Thus, we have shown that the observed deformation in the current density profile was localized inside the island O point.

In conclusion, we have demonstrated the dynamics of the current density profile associated with magnetic island formation in JT-60U. As the island grew, we observed flattening of the current density profile at the island and its subsequent transition from flat to hollow at the resonant surface. This deformed structure gradually diminished with the shrink and disappearance of the island. We also observed that the fluctuation of local poloidal magnetic field is correlated with the island rotation. This indicates that the observed deformation of the current density profile at the island is localized at the island O point. Our observations are an experimental proof of the tearing mode process that theories have predicted. Presently, we have not determined the linear stability index of the tearing mode Δ' from the measured current density profile. The classical onset of tearing modes will be investigated with an appropriate MHD stability code in future work.

The authors thank M. Shimada, T. Ozeki, N. Hayashi, and Y. Ishii for helpful discussions.

[1] H. P. Furth, E. J. Killeen, and M. N. Rosenbluth, Phys. Fluids **6**, 459 (1963).
[2] R. Carrera, R. D. Hazeltine, and M. Kotschenreuther, Phys. Fluids **29**, 899 (1986).
[3] A. Gude *et al.*, Nucl. Fusion **39**, 127 (1999).
[4] Sanae-I. Itoh *et al.*, Phys. Rev. Lett. **91**, 045003 (2003).
[5] D. P. Brennan *et al.*, Phys. Plasmas **9**, 2998 (2002).
[6] V. J. Simic *et al.*, Phys. Fluids B **5**, 1576 (1993).
[7] H. Soltwisch and H. R. Koslowski, Plasma Phys. Controlled Fusion **39**, A341 (1997).
[8] W. X. Ding *et al.*, Phys. Rev. Lett. **90**, 035002 (2003).
[9] T. Fujita *et al.*, Fusion Eng. Des. **34–35**, 289 (1997).
[10] E. Poli *et al.*, Phys. Rev. Lett. **88**, 075001 (2002).
[11] C. B. Forest *et al.*, Phys. Rev. Lett. **79**, 427 (1997).
[12] T. Oikawa *et al.*, Nucl. Fusion **41**, 1575 (2001).
[13] G. Kurita *et al.*, Nucl. Fusion **34**, 1497 (1994).